Biochemical and Biophysical Research Communications 405 (2011) 107–111

Contents lists available at ScienceDirect

Biochemical and Biophysical Research Communications

journal homepage: www.elsevier.com/locate/ybbrc

Solution X-ray scattering study of a full-length class A penicillin-binding protein

P. Macheboeuf [a,*,1], M. Piuzzi [b,1], S. Finet [c,d], F. Bontems [b], J. Pérez [e], A. Dessen [a], P. Vachette [f,*]

[a] Institut de Biologie Structurale, Bacterial Pathogenesis Group, UMR 5075 (CEA, CNRS, Univ. Joseph Fourier-Grenoble I) Grenoble, France
[b] ICSN, CNRS UPR 2301, 91198 Gif-sur-Yvette Cedex, France
[c] IMPMC, CNRS UMR 7590 4 place Jussieu, 75252 Paris Cedex, France
[d] IMPMC, UPMC UMR 7590 4 place Jussieu, 75252 Paris Cedex, France
[e] Synchrotron SOLEIL, BP 48, 91192 Gif-sur-Yvette Cedex, France
[f] IBBMC, Université Paris Sud CNRS UMR8619, bât. 430, F-91405 Orsay Cedex, France

ARTICLE INFO

Article history:
Received 22 December 2010
Available online 7 January 2011

Keywords:
Penicillin binding protein
Glycosyltransferase
Small angle X-ray scattering
Bacterial pathogenesis

ABSTRACT

Penicillin binding proteins (PBPs) catalyze essential steps in the biosynthesis of peptidoglycan, the main component of the bacterial cell wall. PBPs can harbor two catalytic domains, namely the glycosyltransferase (GT) and transpeptidase (TP) activities, the latter being the target for β-lactam antibiotics. Despite the availability of structural information regarding bi-functional PBPs, little is known regarding the interaction and flexibility between the TP and GT domains. Here, we describe the structural characterization in solution by small angle X-ray scattering (SAXS) of PBP1b, a bi-functional PBP from *Streptococcus pneumoniae*. The molecule is present in solution as an elongated monomer. Refinement of internal coordinates starting from a homology model yields models in which the two domains are in an extended conformation without any mutual contact compatible with the existence of restricted mobility.

1. Introduction

The bacterial peptidoglycan is a net-like structure formed by polymerized *N*-acetyl muramic acid and *N*-acetyl glucosamine units, linked together via pentapeptides. It is involved in the maintenance of bacterial shape and the control of internal pressure and must be resynthesized during cell division and elongation processes. Notably, a weakened peptidoglycan can lead to cell lysis and death [1,2]. The last steps of peptidoglycan biosynthesis involve the polymerization of sugar units by glycosyltransfer (GT) and the cross-linking of sugar chains via peptide bonds by transpeptidation (TP) activities [3]. Both enzymatic activities are carried by high molecular mass (HMM) Penicillin binding proteins (PBPs) that are classified as class A molecules (containing both GT and TP activities) and class B (carrying only the TP activity) [1,4].

Since the TP domains from HMM and low molecular mass (LMM) PBPs are the targets of β-lactam antibiotics, their structures have been extensively studied [5–13]. The rapid emergence of resistance to antibiotics employed in clinical settings has led to the intensive search for new potential drug targets, including the GT domains of PBPs. The glycosyltransferase activity of PBPs is a target of choice since, like the transpeptidases, it has an essential function in peptidoglycan biosynthesis; in addition, PBPs are located on the periplasmic side of the cell membrane, making the GT domain accessible to small molecules. Moreover, one well characterized inhibitor of the GT activity, the *Streptomyces* natural product moenomycin, is not employed for human use due to its poor absorption properties [14].

Unlike the TP regions of PBPs, the GT domains are difficult to isolate and to study from a biochemical and structural point of view due to their hydrophobic character. Considerable efforts have been undertaken to purify stable forms of class A PBPs (or their isolated GT domains) in order to perform enzymatic, screening, and structural assays [15–19]. Up to now, two isolated GT domain structures [20,21] and two full-length PBP structures [22,23], the latter including the transmembrane region, have been crystallized and their structures have been solved in the presence of the antibiotic moenomycin. These structures have provided important insights regarding these novel antibiotic development targets. Nevertheless, the interaction and flexibility between the two catalytic domains is not easily understood from the crystallographic structures and still constitute an obstacle in understanding the mechanism of substrate recognition.

In this article we report the structural characterization in solution of PBP1b, a class A PBP from *Streptococcus pneumoniae*, using the combination of SAXS and X-ray crystallography techniques. PBP1b is a bi-functional enzyme that contains a N-terminal GT domain followed by a short linker and a C-terminal TP region. The crystal structure of a truncated form of PBP1b (hereafter desig-

* Corresponding authors. Present address: Unit of Virus and Host Cell Interactions, UMI 3265, Université Joseph Fourier, EMBL, CNRS, Grenoble, France (P. Macheboeuf). Fax: +33 1 69 85 37 15 (P. Vachette).
E-mail addresses: pmache@embl.fr (P. Macheboeuf), patrice.vachette@u-psud.fr (P. Vachette).
[1] These two authors contributed equally to this work.

0006-291X/$ - see front matter © 2011 Elsevier Inc. All rights reserved.
doi:10.1016/j.bbrc.2011.01.003

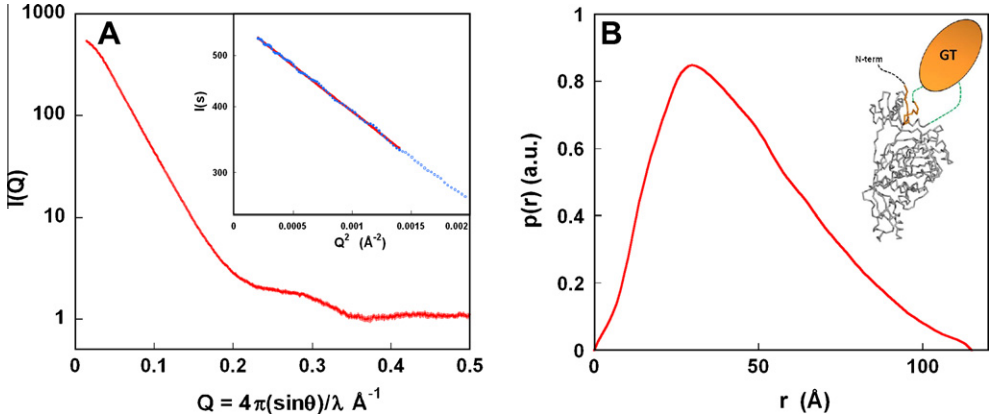

Fig. 1. SAXS pattern of full-length PBP1b: (A) SAXS pattern of PBP1b with associated error bars; inset: Guinier plot. (B) Pair distribution function $p(r)$. Inset: diagram of full-length PBP1b: PBP1b* is shown in ribbon representation with the β-hairpin highlighted in orange and the two linkers in green. (For interpretation of the references to color in this figure legend, the reader is referred to the web version of this article.)

nated as PBP1b*), which lacks most of the GT domain due to the trypsinization protocol employed to generate a soluble form of the enzyme, still harbors a short GT peptide that remained associated to the rest of the molecule even after purification [10]. This peptide lies in close proximity to a hydrophobic funnel near the linker that was previously interpreted as a recognition site for the N-terminal GT domain. It is structured as a β hairpin that extends a three-strand β-sheet from the TP domain. This peptide is followed by a short linker leading to the GT domain, which therefore appears to be connected to PBP1b* through two linkers (see protein diagram in Fig. 1).

Using existing crystal structures of homologue GT domains and full-length enzymes we produced a homology model of *S. pneumoniae* PBP1b. We then determined the arrangement of GT and TP domains by modifying φ–ψ angles in selected regions of the molecule as implemented in a homemade program based on a genetic algorithm. In all resulting conformations the GT domain appears to be located on top of the previously identified surface hydrophobic patch with no other contact between the two domains than the two linkers. This suggests that GT and TP domains may display some relative flexibility although any such motion would be of restricted amplitude due to the twofold connection between them. This result comforts the hypothesis that the modifications in relative positioning of PBP domains could play notable roles in the peptidoglycan formation, including partner recognition or ligand binding.

2. Materials and methods

2.1. Protein purification

The soluble full-length PBP1b containing residues Gly 74 to Pro 791 was expressed and purified as described previously [10]. The GST-PBP1b fusion protein was treated with Tev protease at a 1:100 ratio, dialyzed into glutathione-free buffer and reloaded onto a glutathione column in order to remove the contaminating tag. The protein sample was next dialyzed into 50 mM Tris–HCl, pH 8.0, 20 mM NaCl, 1 mM EDTA and loaded onto an anion exchange column (GE Healthcare). The sample was then loaded onto a size exclusion column in 20 mM HEPES, pH 7.0, 100 mM NaCl, 1 mM EDTA.

2.2. Small angle X-ray scattering (SAXS) measurements and data analysis

SAXS patterns were recorded on the undulator beamline ID02 at the ESRF (Grenoble, France), using a CCD detector coupled to an X-ray image intensifier [24]. Scattering intensities were recorded over the angular range $Q_{min} = 0.013$ Å^{-1}, $Q_{max} = 0.5$ Å^{-1}, where $Q = 4\pi(\sin\theta)/\lambda$ is the momentum transfer, and $\lambda = 0.995$ Å is the wavelength of the X-rays. Ten frames (20 for buffers) of 0.3 s exposure each separated by a 5 s pause were recorded for each protein solution and buffer alike. Between successive frames, fresh solution was pushed into the beam using an automated syringe connected to a quartz capillary of ≈2 mm diameter under vacuum containing the solution. All frames were checked for radiation damage (none was found).

Protein solutions in 50 mM HEPES pH 7.0, 100 mM NaCl, 1 mM EDTA were studied over the concentration range 1.7–12.7 mg/ml. Smaller angle data at 1.7 mg/ml were merged with larger angle data at 12.7 mg/ml to yield a final composite curve that was used in subsequent analysis. Scattering from a 2 mg/ml lysozyme solution was recorded and used for molecular mass calibration.

The radius of gyration and the intensity at the origin were calculated using Guinier law

$$\ln[I(Q)] = \ln[I(0)] - (R_g^2/3)Q^2 \quad (1)$$

over the angular range $QR_g < 1.3$ [25]. The pair distribution function was determined using the indirect Fourier transform approach as implemented in the Gnom program [26]. Alternative estimates of the radius of gyration and the intensity at the origin were derived from the calculated $p(r)$.

2.3. GT domain ab initio modeling

The program BUNCH implements a combination of *ab initio* and rigid body modeling using the high-resolution structures of rigid domains of the protein when available [27]. It was used to model *ab initio* the conformation and position of both the N-ter end and the missing GT domain with respect to the known PBP1b* structure. The program describes the missing parts as chains of dummy residues (DR) attached to the N-terminus of the β-hairpin and to both the C-terminus of the β-hairpin and the N-terminus of the TP domain, respectively. Regarding the GT domain, it imposes that the missing part adopts a compact, globular, conformation by constraining the radius of gyration of the DR chain to be close to that of a typical globular protein containing the same number N of residues approximated by the expression $3^3\sqrt{N}$ [27].

2.4. PBP1b modeling using homology model and SAXS data

2.4.1. Homology modeling

The program Modeller [28] was used to derive a model for the full-length molecule using the structure of *Aquifex aeolicus* PBP1a

(PDB code 2oqo) and a composite structure containing the GT domain of *Staphylococcus aureus* PBP2 (PDB code 2olu) linked to the structure of PBP1b* (PDB code 2BG3); this hybrid structure contains the 15 residue long GT peptide from PBP1b*. The 2 PDB structures and the sequence alignment of the chimera, PBP1a and the full-length PBP1b were used to create a model that satisfied restraints from the known related structures and was optimized by molecular dynamics and simulated annealing. The sequence alignment between the composite structure and PBP1b or PBP1a shows 35% and 46% similarity, respectively, taking into account their GT domains. The scattering intensity curve of the resulting model was calculated from atomic coordinates using Crysol [29]. The various models were displayed using the program Pymol (http://www.pymol.org).

2.4.2. Data fitting using φ, ψ angles

We originally designed a modeling program, to determine the global structure of modular proteins from homology models of their domains in the presence of SAXS and/or NMR data using a genetic algorithm [30]. Most modular or multi-domain proteins exhibit a linear succession of domains connected by linkers that are amenable to study using this approach [31]. As already mentioned, the glycosyltransferase domain is connected via two linkers to the transpeptidase domain. To handle this specific configuration we introduced a new operator (the extended local mutation) that made possible the displacement of GT domain with respect to TP domain without breaking the linkers. A residue of the first linker was randomly chosen and a small rotation around its N-Cα (φ dihedral angle) or Cα-C (ψ dihedral angle) bond was applied to all residues of the GT domain. The geometry of the second linker was then adjusted by minimization thereby resealing the polypeptide chain.

PBP1b was divided into five regions: PBP1b* comprising the TP domain together with the attached β-hairpin (residues 101–119 and 336–791), GT domain (residues 128–322), the first (residues 120–127) and second (residues 323–335) linkers, and the N-terminal segment (residues 74–100). The two domains were not altered in any way; no mutation operator was directly applied to them. The glycosyltransferase domain was displaced as a rigid body with respect to the transpeptidase domain through the application of the extended local mutation operator between the two linkers.

A set of initial structures was generated and randomly dispatched into 43 families of 25 models each. Each family was submitted to 50 expansion-selection cycles and the selection pressure was gradually increased during the process. The agreement between the structures and the SAXS curve was measured by a χ^2 calculated in the Q-range [0.018 $Å^{-1}$, 0.35 $Å^{-1}$].

The calculated curves were obtained using Crysol with a maximal number of 25 harmonics and a Fibonacci order of 18 while keeping the density contrast of the solvation shell fixed at 0.03 $e^- Å^{-3}$. Calculated values were scaled to experimental data using the sum of intensities over the fitting Q-range. An entirely rewritten version of the modeling program, which includes new algorithms and a user-friendly graphical interface, will soon be released (Evrard et al., in preparation).

2.4.3. SAXS models clustering

Models were clustered according to different criteria making use of scripts written in Python for use in Pymol. Prior to clustering, all models were superimposed via their TP domain left unchanged during the refinement process. The first criterion used was the distance between centers of mass of GT domains with a cut-off value at 12 Å. We also used the fraction of main-chain atoms of a GT model within 5 Å of at least one main-chain atom of another GT model as a crude approximation of volume overlap. Clustering was performed using a cut-off value of 50%. Finally, models were clustered according to the rmsd between Cα atoms of GT domains using a cut-off distance of 12 Å.

3. Results and discussion

3.1. Global structural parameters

The scattering pattern obtained after splicing of smaller (dilute solution) and larger angle data (more concentrated solution) is shown in Fig. 1A (dots) while the corresponding distance distribution function $p(r)$ is shown in Fig. 1B and the Guinier plot in Fig. 1A inset. The values of the radius of gyration R_g derived from Guinier law is 34.8 ± 0.3 Å, in good agreement with that derived from the $p(r)$ function (35.4 ± 0.3 Å). Using lysozyme as a reference sample, the molecular mass for the full-length PBP1b derived from the intensity at the origin was estimated to be about 72 kDa, in agreement with the known molecular mass derived from the amino acids sequence (78.4 kDa), thereby ruling out any significant aggregation. The value of the maximal diameter D_{max} of the molecule is 115 ± 5 Å. The asymmetric shape of the $p(r)$ function with a maximum at r = 29 Å, much smaller than $D_{max}/2$, is typical of an elongated particle.

3.2. Ab initio GT models

Missing residues were modeled as chains of dummy residues (DR) as implemented in the program Bunch. The β-hairpin (residues 105–119) seen anchored in the crystal structure of PBP1b* was preserved and two parts were modeled as DR chains: the unconstrained 33 N-ter residues and the GT domain comprising 217 residues assumed to adopt a globular conformation. A series of models were obtained, whose scattering pattern nicely fitted experimental data with χ values close to 1. Two models are presented in Fig. 2 in which each DR is represented by a sphere of radius 3.2 Å whose volume is equal to the average volume of an amino-acid residue, i.e. about 140 $Å^3$. The N-terminal stretch is seen exposed to the solvent with a highly variable orientation with respect to the rest of the molecule. In contrast, the GT domain appears close to the TP domain, with no direct contact with the TP domain other than the two linkers. Although not uniquely determined, the domains are not widely distributed with distances between centers of mass of about 15 Å reaching 30 Å for the two most distant models.

3.3. φ and ψ angles model refinement

Recently, crystal structures of two isolated GT domains [20,21] and of two full-length PBP proteins [22,23] were determined. This prompted us to produce a homology model for the full-length molecule by Modeller using a hybrid structure containing the GT domain of *S. aureus* PBP2 and the TP domain from PBP1b*, the structure of *A. aeolicus* PBP1a and the sequence alignment of PBP1b, PBP1a and the chimera. The presence in our crystal structure of the short GT peptide bound to the TP domain brought in very useful constraints that helped Modeller to converge toward a quasi "unique" solution (blue in Fig. 3).

The calculated scattering curve from the homology model, although similar to the experimental data, exhibited significant differences with a χ value of 4.3 over the Q-range [0.013 $Å^{-1}$, 0.35 $Å^{-1}$] (blue in Fig. 4). Runs from our modeling program were performed leading to resulting models whose scattering patterns exhibited a variable degree of agreement with experimental data, with χ values ranging from 0.8 to 1.8, a marked improvement with respect to the initial Modeller model. Twelve models (*ca.* 30%) with a χ value lower or equal to 1 were further considered and superim-

Fig. 2. Bunch modeling of the missing N-ter end and GT domain. The crystal structure of the TP domain is shown in cartoon representation deep teal while two Bunch models for the GT domain and associated N-ter are shown in light orange and salmon. The dummy residues are represented as spheres of radius 3.2 Å (see text for details). (For interpretation of the references to color in this figure legend, the reader is referred to the web version of this article.)

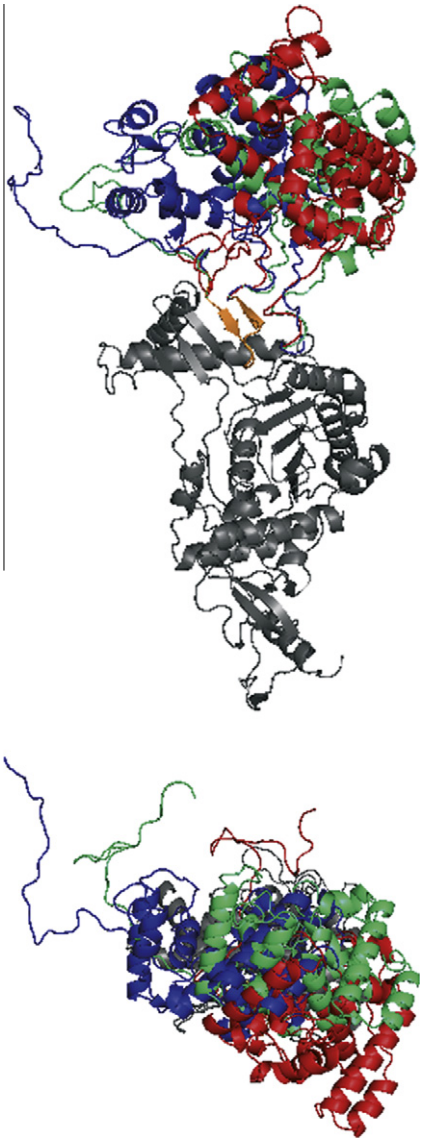

Fig. 3. Models derived from the Modeller homology domain using our modeling program along two orthogonal views. Grey: TP domain common to all models; GT domain and N-ter end are shown in different colors; blue: original model from Modeller; red: best fitting model; green: second best fit model close to the center of the cluster. The β-hairpin is highlighted in orange. (For interpretation of the references to color in this figure legend, the reader is referred to the web version of this article.)

posed using the transpeptidase domain. Two models are shown in Fig. 3 together with the original Modeller model. Their scattering patterns are shown in Fig. 4 panel A while the reduced residuals with respect to experimental data are shown in panel B.

Clustering analysis using distances between centers of mass of GT domains (see Section 2 for details) allowed us to partition our 12 models into one major cluster comprising 10 models and 2 outliers. Clustering using the volume overlap criterion yielded identical results, showing that 80% of all models exhibited more than 50% volume overlap in a position close to that predicted by Bunch. Finally rmsd clustering of all members of the previously defined cluster selected 8 of them with an rmsd smaller or equal to 12 Å with the remaining two displaying much larger values in the range [15 Å, 35 Å] and [25 Å, 50 Å], respectively. These last two, although having a large volume overlap with other models, were in markedly different orientations around the long axis of the molecule.

The fact that different models could be found is no proof of mobility, it simply reflects the finite amount of structural information in our data that are compatible with a manifold of models. However, all models share some common features such as the location of the GT domain at one end of the molecule and the absence of contacts between GT and TP domains besides the linker regions. This observation opens up the possibility that the two domains present some relative mobility. This seems to be in line with observations of large amplitude flexibility of GT and TP domains in crystal structures of *S. aureus* PBP2 reported in [22,32]. The differences between the various conformers can be described in terms of rigid-body movements of domains. Using the domain motion analysis program DynDom [33], the authors report a relative domain movement in the order of 100° and 3–4 Å between chains from PBP2Δ and the apoenzyme form. Could PBP1b also exhibit large amplitude movements of domains in solution? Our data and the resulting models provide us with some information in that respect. Indeed, all conformations appear to be more extended than the conformation of PBP2 complexed with moenomycin (2OLV pdb file), the most axial conformation exhibited by PBP2 (see Fig. 2a in [32]). It follows that if PBP1b explored a large conformational space comparable to that sampled by PBP2 in the various crystal structures, sharply bent conformations could only represent a very minor fraction of the ensemble for the global distribution to account for the experimental data. In conclusion, although the molecule most likely exhibits interdomain mobility around the two linkers between GT and TP domains, our experimental data suggest that its amplitude is restricted, at least in the absence of any partner or ligand, to a conformational space not much broader than the

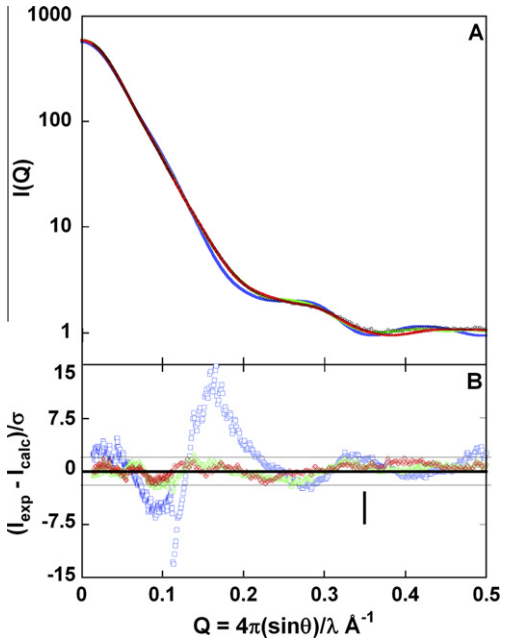

Fig. 4. Scattering patterns of models derived from the Modeller homology model using our modeling program. (A) Calculated scattering patterns of models are shown as continuous lines superimposed on the experimental scattering intensities shown with associated error bars. Black dots: experimental data; grey line: homology model from Modeller; red line: best fit to SAXS data; blue line: pattern of the second best fit model close to the cluster center; (B) reduced residuals of the least-squares fits ($(I_{exp} - I_{calc})/\sigma_{exp}$) shown on a linear scale. Same color code as in panel A. The vertical bar at $Q = 0.35$ Å^{-1} shows the outer boundary of the data included in the fit. Two horizontal lines define the $\pm 2\sigma$ range. (For interpretation of the references to color in this figure legend, the reader is referred to the web version of this article.)

solution space sampled by our models. The latter, which all account individually for the scattering data, are therefore likely to provide a good picture of the unliganded molecule in solution. This is a direct consequence of the presence of the β-hairpin anchored in the TP domain that appears to play a significant role in the protein structure by allowing GT and TP domains to undergo limited movements that could be advantageous for the activity of a bifunctional enzyme in a crowded environment.

Acknowledgments

We thank the ESRF (Grenoble, France) for the provision of beamtime and excellent facility. This research was supported by funding from CNRS and CEA. P. Macheboeuf was a recipient of a CFR fellowship from the Commissariat à l'Énergie Atomique and M. Piuzzi was the recipient of a doctoral fellowship from ICSN (UPR2301 CNRS).

References

[1] J.V. Höltje, Growth of the stress-bearing and shape-maintaining murein sacculus of *Escherichia coli*, Microbiol. Mol. Biol. Rev. 62 (1998) 181–203.
[2] W. Vollmer, D. Blanot, M.A. de Pedro, Peptidoglycan structure and architecture, FEMS Microbiol. Rev. 32 (2008) 149–167.
[3] P. Matteï, D. Neves, A. Dessen, Bridging cell wall biosynthesis and bacterial morphogenesis, Curr. Opin. Struct. Biol. 20 (2010) 749–755.
[4] P. Macheboeuf, C. Contreras-Martel, V. Job, O. Dideberg, A. Dessen, Penicillin binding proteins: key players in bacterial cell cycle and drug resistance processes, FEMS Microbiol. Rev. 30 (2006) 673–691.
[5] Y. Chen, W. Zhang, Q. Shi, D. Hesek, M. Lee, S. Mobashery, et al., Crystal structures of penicillin-binding protein 6 from *Escherichia coli*, J. Am. Chem. Soc. 131 (2009) 14345–14354.
[6] C. Contreras-Martel, V. Job, A.M. Di Guilmi, T. Vernet, O. Dideberg, A. Dessen, Crystal structure of penicillin-binding protein 1a (PBP1a) reveals a mutational hotspot implicated in beta-lactam resistance in *Streptococcus pneumoniae*, J. Mol. Biol. 355 (2006) 684–696.
[7] C. Contreras-Martel, C. Dahout-Gonzalez, A.D.S. Martins, M. Kotnik, A. Dessen, PBP active site flexibility as the key mechanism for beta-lactam resistance in *pneumococci*, J. Mol. Biol. 387 (2009) 899–909.
[8] V. Job, R. Carapito, T. Vernet, A. Dessen, A. Zapun, Common alterations in PBP1a from resistant *Streptococcus pneumoniae* decrease its reactivity toward beta-lactams: structural insights, J. Biol. Chem. 283 (2008) 4886–4894.
[9] D. Lim, N.C.J. Strynadka, Structural basis for the beta lactam resistance of PBP2a from methicillin-resistant *Staphylococcus aureus*, Nat. Struct. Biol. 9 (2002) 870–876.
[10] P. Macheboeuf, A.M. Di Guilmi, V. Job, T. Vernet, O. Dideberg, A. Dessen, Active site restructuring regulates ligand recognition in class A penicillin-binding proteins, Proc. Natl Acad. Sci. USA 102 (2005) 577–582.
[11] C. Morlot, L. Pernot, A. Le Gouellec, A.M. Di Guilmi, T. Vernet, O. Dideberg, et al., Crystal structure of a peptidoglycan synthesis regulatory factor (PBP3) from *Streptococcus pneumoniae*, J. Biol. Chem. 280 (2005) 15984–15991.
[12] R.A. Nicholas, S. Krings, J. Tomberg, G. Nicola, C. Davies, Crystal structure of wild-type penicillin-binding protein 5 from *Escherichia coli*: implications for deacylation of the acyl-enzyme complex, J. Biol. Chem. 278 (2003) 52826–52833.
[13] E. Sauvage, F. Kerff, E. Fonzé, R. Herman, B. Schoot, J.P. Marquette, et al., Cell. Mol. Life Sci. 59 (2002) 1223–1232.
[14] R.C. Goldman, D. Gange, Inhibition of transglycosylation involved in bacterial peptidoglycan synthesis, Curr. Med. Chem. 7 (2000) 801–820.
[15] D.S. Barrett, L. Chen, N.K. Litterman, S. Walker, Expression and characterization of the isolated glycosyltransferase module of *Escherichia coli* PBP1b, Biochemistry 43 (2004) 12375–12381.
[16] D. Barrett, C. Leimkuhler, L. Chen, D. Walker, D. Kahne, S. Walker, Kinetic characterization of the glycosyltransferase module of *Staphylococcus aureus* PBP2, J. Bacteriol. 187 (2005) 2215–2217.
[17] A.M. Di Guilmi, A. Dessen, O. Dideberg, T. Vernet, Functional characterization of penicillin-binding protein 1b from *Streptococcus pneumoniae*, J. Bacteriol. 185 (2003) 1650–1658.
[18] J. Offant, F. Michoux, A. Dermiaux, J. Biton, Y. Bourne, Functional characterization of the glycosyltransferase domain of penicillin-binding protein 1a from *Thermotoga maritima*, Biochim. Biophys. Acta 1764 (2006) 1036–1042.
[19] M. Terrak, M. Nguyen-Distèche, Kinetic characterization of the monofunctional glycosyltransferase from *Staphylococcus aureus*, J. Bacteriol. 188 (2006) 2528–2532.
[20] H. Heaslet, B. Shaw, A. Mistry, A.A. Miller, Characterization of the active site of *S. aureus* monofunctional glycosyltransferase (Mtg) by site-directed mutation and structural analysis of the protein complexed with moenomycin, J. Struct. Biol. 167 (2009) 129–135.
[21] Y. Yuan, D. Barrett, Y. Zhang, D. Kahne, P. Sliz, S. Walker, Crystal structure of a peptidoglycan glycosyltransferase suggests a model for processive glycan chain synthesis, Proc. Natl Acad. Sci. USA 104 (2007) 5348–5353.
[22] A.L. Lovering, L.H. de Castro, D. Lim, N.C.J. Strynadka, Structural insight into the transglycosylation step of bacterial cell-wall biosynthesis, Science 315 (2007) 1402–1405.
[23] M. Sung, Y. Lai, C. Huang, L. Chou, H. Shih, W. Cheng, et al., Crystal structure of the membrane-bound bifunctional transglycosylase PBP1b from *Escherichia coli*, Proc. Natl Acad. Sci. USA 106 (2009) 8824–8829.
[24] D. Pontoni, T. Narayanan, A.R. Rennie, High-dynamic range SAXS data acquisition with an X-ray image intensifier, J. Appl. Crystallogr. 35 (2002) 207–211.
[25] A. Guinier, G. Fournet, in: Small Angle Scattering of X-Rays, Wiley, New York, 1955.
[26] D.I. Svergun, Determination of the regularization parameter in indirect-transform methods using perceptual criteria, J. Appl. Crystallogr. 25 (1992) 495–503.
[27] M.V. Petoukhov, D.I. Svergun, Global rigid body modeling of macromolecular complexes against small-angle scattering data, Biophys. J. 89 (2005) 1237–1250.
[28] A. Fiser, A. Sali, Modeller: generation and refinement of homology-based protein structure models, Methods Enzymol. 374 (2003) 461–491.
[29] D. Svergun, C. Barberato, M.H.J. Koch, CRYSOL – a program to evaluate X-ray solution scattering of biological macromolecules from atomic coordinates, J. Appl. Crystallogr. 28 (1995) 768–773.
[30] F. Mareuil, C. Sizun, J. Perez, M. Schoenauer, J. Lallemand, F. Bontems, A simple genetic algorithm for the optimization of multidomain protein homology models driven by NMR residual dipolar coupling and small angle X-ray scattering data, Eur. Biophys. J. 37 (2007) 95–104.
[31] P. Aliprandi, C. Sizun, J. Perez, F. Mareuil, S. Caputo, J. Leroy, et al., S1 ribosomal protein functions in translation initiation and ribonuclease RegB activation are mediated by similar RNA-protein interactions: an NMR and SAXS analysis, J. Biol. Chem. 283 (2008) 13289–13301.
[32] A.L. Lovering, L. De Castro, N.C.J. Strynadka, Identification of dynamic structural motifs involved in peptidoglycan glycosyltransfer, J. Mol. Biol. 383 (2008) 167–177.
[33] S. Hayward, H.J. Berendsen, Systematic analysis of domain motions in proteins from conformational change: new results on citrate synthase and T4 lysozyme, Proteins 30 (1998) 144–154.